We are IntechOpen,
the world's leading publisher of
Open Access books
Built by scientists, for scientists

4,800
Open access books available

122,000
International authors and editors

135M
Downloads

Our authors are among the

154
Countries delivered to

TOP 1%
most cited scientists

12.2%
Contributors from top 500 universities

CLARIVATE ANALYTICS
BOOK CITATION INDEX INDEXED

WEB OF SCIENCE™

Selection of our books indexed in the Book Citation Index
in Web of Science™ Core Collection (BKCI)

Interested in publishing with us?
Contact book.department@intechopen.com

Numbers displayed above are based on latest data collected.
For more information visit www.intechopen.com

Intelligent Assisting Tools for Endodontic Treatment

Csaba Dobo-Nagy and Balazs Benyo

Abstract

The integration of image processing in novel systems bids fair to significantly improve the endodontic practice in the near future. Also, the attempt to automatically locate and classify the root canals may result in significantly decreased chair time for both the patient and the practitioner. We focus on the shapes of human root canals and their automatic classification, methods for automatic processing, and center line identification of tooth root canal as defined previously. We introduce some micro-computed tomography image analysis methods possible for clinical implementation of cone beam computed tomography image analysis in endodontics and limitations of novel techniques. In this chapter, we present our results of segmentation and root canal identification of cone beam computed tomography images.

Keywords: image processing, skeleton extraction, cone beam computed tomography, human root canal geometry, fuzzy relations

1. Introduction

Tooth development is a more complex biological process moderated by a series epithelial and mesenchymal interactions [1]. Every developed root canal has its own individual form; therefore, visualizing and understanding root canal systems are essential for successful root canal treatment (**Figure 1**). Classifications were formulated on basis of: number and relations of canals in a single root, cross-sectional forms, and the curvature along the long axis of the main root canal [2]. Alteration of normal odontogenesis causes developmental anomalies in roots. Depending on the stage of tooth development, various anomalies either in root or root canal number or size or shape can occur [1]. The most common human root malformations include: dilacerations, taurodontism, root fusion, dens invaginatus, and C-shape canals. A new complex system has been developed for classifying root morphology, the main root canal system in relation to accessory canals and root canal anomalies [3]. A new coding system was also introduced to provide more comprehensive information on the morphological features of a specific tooth, root, and canal within a single code.

These complex data characterizing roots' inner and outer forms were provided by micro-computed tomography (μCT) technology. This technology opens a new world for fine visualization and micro-morphological characterization of dental root canals for endodontists. All of the aforementioned necessary morphological information was gained from μCT image set collected from extracted teeth scans.

Figure 1.
Micro-CT visualization of root canal system of an upper molar from mesial view.

Clinical adaptation of this information is still limited to a few characteristics namely imaging of the outer shape of root, number and aspect of roots and root canals, main canal path, and visualization of anomalies and pathology. These limitations are due to the lower resolution provided by cone-beam computed tomography (CBCT) technology; however, information from CBCT imaging has been revolutionary, improving the clinical endodontic practice.

2. Typical shapes of human root canals and their automatic classification

On basis of serial histological sections, Hess [4] gave a detailed description about a high variety of human dental root canals. Fine detailed forms of root canals

were reported demonstrating the more complexity and uniformity of a single root canal system. This excellent detailed description method is extremely time consuming and clinically irrelevant since endodontists require information on anatomy of a given root canal prior the endodontic treatment. By involving intraoral radiography, endodontists of the everyday practice collected information from periapical radiographs, mainly from clinical views. Two-dimensional radiographic image of the root canal system is hardly reliable for collecting information on the real root canal anatomy. Therefore, endodontists use not only a bucco-lingual but eccentric views, as well. Resolution and the two-dimensional nature of intraoral radiographs are the main limitations of this worldwide used technique. Intraoral radiographs provide one view information on the number of main root canals and their curvatures (mainly in the coronal and middle levels of root) but not on their cross-sectional form. On intraoral radiographs, accessory canals, fine contours of canal wall-like fins, and intricacy or isthmuses between roots are hardly detected. At this level of technology, researchers formulated classifications focusing on the curvature along the long axis of the main root canal being the most useful information gained from this technique [5, 6]. These classifications distinguish straight, gradual curve, severe curve, and bayonet forms. According to the location along the entire canal length, they defined apical or middle level (sickle shape) curvatures. Attempts had been made to use measurement for determination of canal curvatures beginning at the 1970s. All of the classifications were based on angle measurement of curvatures [7]. These authors recognized that single datum (angle measurement) is not appropriate to describe the course of canal curvature. Therefore, they used supplementary data beyond the angle measurement, for example, radius quotient [8] or radius measurement [6]. These supplementary data were meant to define localization (apical or middle level) of curvatures. The first automatic classification was introduced in 1995 [2]. Their method was based on manually defined points of imaginary root canal axis from planar radiographs; however, the classification process had been automatized. They used fourth degree polynomial approximation to the defined points of the imaginary canal axis. Then the curvature function of polynomials was calculated. Characterization of curvature functions was made the basis of automatic classification. The sign, values, and their percentage distribution along the entire length of canal were concerned (**Figure 2**). This automatic classification was able to distinguish four types of root canal forms, for example, straight (I-form), apically curved (J-form), gradually curved (C-form), and multicurved (S-form) canals.

Endodontists drew up demand on three-dimensional cleaning, shaping, and obturation of the root canal system [9]. By the last decade of the twentieth century, technology had developed to a level that it could approach the three-dimensional root canal shape in certain ways. Volume and diameters of root canals were able to be calculated by introducing computer-assisted tomography [10]. From root canal serial sections, computerized wireframe images were built up [11]. Detailed spatial reconstruction of root canal system was made by magnetic resonance microscopy [12]. Micro-computed tomography was introduced in endodontic research [13]. Before the CBCT use in dentistry, a research group provided a computer-graphics description of three-dimensional root canal axis [14]. They manually determined relevant points of root canals on Monge image pairs and calculated three-dimensional polynomial curve of root canal axis from each well-ordered Monge image pairs.

On the basis of the current state of technology, the presentation of three-dimensional axis of root canals or automatic classification of three-dimensional axes seems to provide useful information for endodontists for carrying out proper root canal treatment.

sample No.: 23   30x magnification

ПΠ

correlation: 0.9999938

200x magnification of curvature values
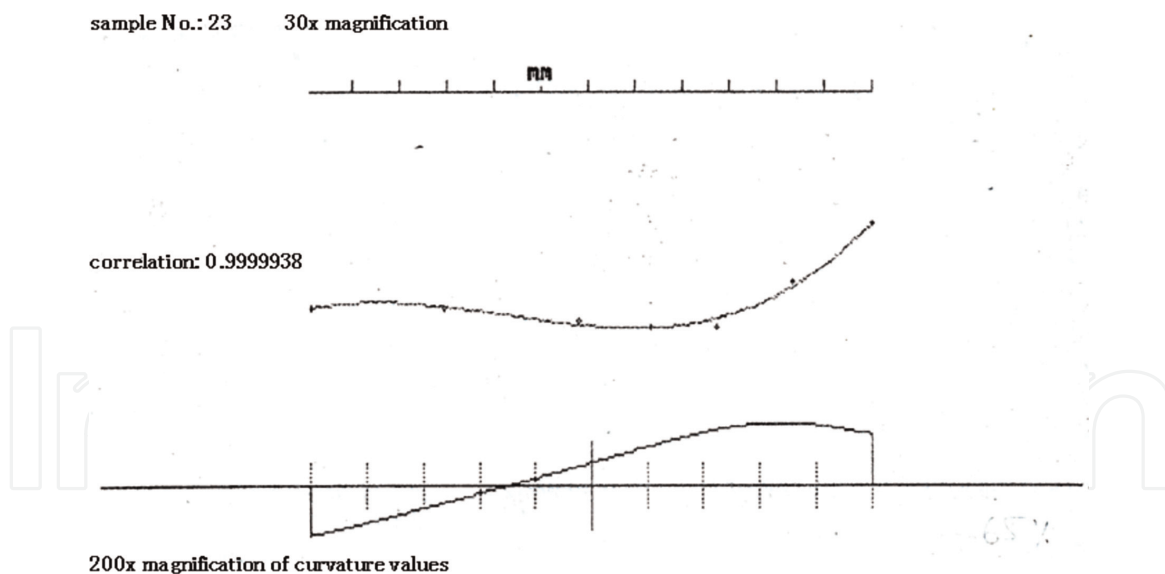
Figure 2.
Two-dimensional curvature of a single S-form root canal. Root canal axis plotted by fourth degree polynomial function approximation (above). Below the curvature function in relation of the percentage of the root length is shown. Characteristics of this form are a significant amount of both positive and negative values of curvature.

3. Image enhancement filters image classifications and segmentation methods for automatic processing

The individual root canal configuration and shape of patients, severely curved root canals, or multi-rooted teeth pose serious challenges in the automatic or semi-automatic extraction of the root canal and the identification of its center line.

3D medical imaging techniques (µCT, CBCT, etc.) enable recording 3D representation of the teeth, in which data can be processed by image processing methods to extract the shape of the root canal. Several alternative solutions have been developed for this specific problem depending on the recorded data which can be generated by different imaging modalities.

Stereo digital radiography is a relatively simple imaging modality that can be used for modeling and measurement of root canals. Analui et al. [15] developed a geometric modeling method that can be used by human dentists for the measurement of the root canal parameters. A 3D tooth model can be built using 2D radiographic images by the method suggested by Hong et al. [16]. Root canals can be detected on ultrasonic images by the fuzzy logic based method suggested by Endo et al. [17]. Lee et al. [18] developed a 3D reconstruction software and applied mathematical modeling to measure the 3D canal curvature in maxillary first molars on µCT images. 3D reconstruction algorithms are also developed for different imaging modalities: Willershausen et al. [19] proposed X-ray image-based reconstruction; van Soest et al. [20] processed optical coherence tomography images in their reconstruction method. Virtual reality-based imaging system developed by Germans et al. [21] can be used to visualize the internal surfaces of reconstructed 3D tooth structures and measure the curvature of the root canal. Root canal configuration of the teeth can be identified by the method proposed by Park et al. [22]. The identification method is specialized for the first molars and processes µC images. Quantification of the caries excavation can be solved by the method of Neves et al. [23]. Verma and Love [24] and Yamada et al. [25] proposed methods to evaluate the morphology of the root canal. Kaya et al. [26] specifically studied the root canal changes of the incisors as a result of aging. The effect of manual

instrumentation on the root canal configuration is also investigated by Li et al. [27]. General features and characterization of the root canal is also possible by the modeling tool suggested by Frisardi et al. [28].

Based on this short literature survey, the image processing methods aiming the extraction of the of the root canal center line can be divided into two main phases:

1. *Root canal segmentation phase:* separation of image regions (voxels or pixels depending on the actual representation of the) belonging to the dentine and root canal (endodontium).

2. *Center line identification phase:* reconstruction of the 3D shape of the root canal and identification of the center line.

Basically, there are two general approaches that can be applied in the root canal segmentation phase:

a. Separation of the 3D data sets into a sequence of 2D images, and then processing these 2D slices individually. The information provided by the 3D data set (i.e. similarities of the identified shape and size of the root canal segments) is used only in the subsequent root canal reconstruction phase.

b. Direct processing of the 3D data sets representing the tooth.

The advantage of *approach (a)* is the problem decomposition into several smaller sized image processing steps. This problem decomposition may significantly reduce the execution time of the image processing as the image processing methods generally have relatively high computational complexity making the root canal segmentation time-consuming. The memory consumption of the image processing algorithm can also be efficiently reduced by the problem decomposition as the size of the processed individual data sets is significantly smaller than the original 3D data set. This approach is frequently applied in the case of large 3D data sets (e.g. in the case of μC images) to use the benefits of the above advantages. These 3D data sets are generally high resolution images with relatively good quality. This is an important factor in the selection of the appropriate image processing approach as the high noise/signal ratio may actually hinder the application of *approach (a)*.

The advantage of *approach (b)* is the opportunity to consider the 3D neighborhood of the processed voxel and the opportunity to involve this information into the decision about the membership status of the given voxel. This information is sometimes vital to make an appropriate decision especially in the case of low resolution images where the compensation of the so-called partial volume effect is necessary.

There are several factors that have to be considered by the implementation of both of the approaches. The signal-to-noise ratio is proportional to the X-ray dose applied during the imaging. Due to clinical considerations, the dose is kept minimal [29], and thus, the noise level in the image volumes processed is frequently high. Due to these circumstances, an efficient filtering technique has to be applied to reduce the adverse effect of high frequency noise upon segmentation, without altering or significantly reducing detectable edges. Context sensitive averaging filter proposed in [30] is an efficient tool to perform this operation.

The CT images are gray scale images where the intensity represents the attenuation coefficient measured in Hounsfield unit. The main challenge in the implementation of *approach (a)* is to find the appropriate intensity threshold value for the segmentation. Optimal clustering algorithms, such as the fuzzy c-means

algorithm can be used to define the intensity threshold value in an adaptive way for each 2D slice of the data [31].

The most reasonable algorithm that can be used to implement *approach (b)* is region growing [32]. Region growing algorithms are pixel-based image segmentation methods growing homogeneous regions around the so-called seed points. The approach is very simple; the segmentation algorithm examines neighboring pixels of the initial seed points and determines whether the pixel neighbors meet the so-called homogeneity criterion. The criterion is frequently defined based on the voxel intensities of the examined region. The region is considered to be homogeneous when the standard deviation of the voxel intensities is below a given threshold. However, this approach is relatively sensitive to noise.

High frequency noises can easily result in over-segmentation, i.e., a high number of small regions. Intensity inhomogeneity of images may also cause serious challenges for the classical region growing algorithm as such a noise would avoid the creation of large homogeneous regions.

These bottlenecks of the classical region growing algorithms can be compensated by a fuzzy subset-based region growing method defined as follows. The image volume (X) is defined as a set of voxels: $X = \{x_1, x_2, ..., x_N\}$, where N represents the number of voxels. A *fuzzy subset* of X is defined as a set of ordered pairs:

$$F = \{(x_i, \mu_F(x_i)) | i = 1...N\}, \tag{1}$$

where $\mu_F: X \to [0, 1]$ is called the membership function F in X. We can define a fuzzy relation in X as a fuzzy subset of X^2 written as

$$y = \{((x_i, x_j), \mu_F(x_i, x_j)) | i, j = 1...N\}, \tag{2}$$

with $\mu: X^2 \to [0, 1]$. The so-called α-cut of a fuzzy subset F is the crisp set:

$$X_\alpha^{(F)} = \{x \in X | \mu_F(x) \geq \alpha\}. \tag{3}$$

The fuzzy relation y_α is called a fuzzy link between x_i and x_j, if:

$$\exists \alpha \in (0,1] : \mu_y(x_i, x_j) \geq \alpha. \tag{4}$$

If a fuzzy relation y_α holds over a set $X = \{x_1, x_2, ..., x_N\}$, then we may write $x_i y_\alpha x_j \ \forall x_i, x_j \ X$.

Two elements x_i and x_j of a set X are α-chained, if there exists a sequence of fuzzy linked elements $\xi_1, \xi_2, ..., \xi_k$ in X, such as

$$x_i y_\alpha \xi_1 y_\alpha \xi_2 y_\alpha \cdots y_\alpha \xi_{k-1} y_\alpha \xi_k y_\alpha x_j. \tag{5}$$

In the fuzzy subset-based region growing algorithm, two points will be in the same segment whenever they are α-chained through neighbor voxels. In the case of tooth segmentation, the fuzzy relation allowing the separation of different tissues of tooth hast to be defined, as well as the appropriate value of α that assures the required granularity of detected segments.

The final goal is to separate the root canal from the other tissues of the tooth; thus in the segmented images, the dentine should be seen as a continuous 3D region embedding the region belonging to the root canal. Thus, the similarity between two voxels is simultaneously defined by the difference between their intensity and their distance. This compound relation can be defined similarly to the coefficients of the

context-dependent filter defined in [30]. The resultant definition of the fuzzy relation contains the following product:

$$\mu_y\left(x_i, x_j\right) = \delta_y\left(x_i, x_j\right) \times \sigma_y\left(x_i, x_j\right) \qquad (6)$$

The first term ($\delta_y\left(x_i, x_j\right)$) depends on the distance of the voxels. The second term ($\sigma_y\left(x_i, x_j\right)$) reflects the similarity between the intensity of the given voxels. The above terms are defined according to the following rules:

$$\delta(x_i, x_j) = \frac{1}{\sqrt{1 + \kappa_\delta d(x_i, x_j)}}. \qquad (7)$$

$$\sigma(x_i, x_j) = \frac{1}{\sqrt{1 + \kappa_\sigma |\log \frac{v(x_i)}{v(x_j)}|}}. \qquad (8)$$

where κ_δ and κ_σ are the parameters that enable tailoring the behavior of the segmentation algorithm.

4. Challenges and methods of center line identification of tooth root canal

3D curve skeletons are the collection of internal points (voxels) of an object that have the same distance from at least two boundary (surface) points of the object. Thus the center line of the root canal can be approximated by the curve skeleton of the root canal. Curve skeletons preserve the object's topology and clearly represent the hierarchy of the component objects. This is essential in the detection of root canal bifurcations. Dental root canal identification requires an appropriate curve skeleton extraction method that can yield smooth curves and is insensitive to slight changes of the object's boundary.

3D curve skeletons [33] are frequently used to approximate the topology of tubular structures such as dental root canals. A high number of curve skeleton extraction methods are published. Most of the methods are iterative algorithms that remove points (voxels) from the original volume to extract the skeleton. The thinning and boundary propagation method removes those surface points—called simple points—whose deletion will not change the topology. The topology criteria are tested by a 3D extension of the hit-or-miss transform [34, 35]. The distance field-based methods use the distance of the internal voxels (points) from the closest boundary (surface) point. The curve skeleton is approximated by the selection of the local maximums of these distance measures identifying the ridges of this distance field [36]. Geometric model-based approaches generally use a graph-based representation of the objects and create the medial lines in the form of connected curves [37]. The so-called potential field-based method applies the generalized form of the electrostatic field calculation methods known from physics [38]. The method places point charges to all the surface (boundary) voxels (points) and calculates the electrostatic field generated by these point charges. The calculated electrostatic field is used to extract a hierarchical structure composed of critical and saddle points of the field defining the curve skeleton of the object.

5. Results of segmentation and root canal identification of cone beam computed tomography images

The 3D CBCT images are frequently processed by slices as it is described in the previous sections. Typical slices of CBCT images are shown in **Figure 3**, where we can find the cross section of the same tooth on different sections of the root canal.

Due to the CBCT geometry and the low-dose imaging, the 2D images are noisy, generally affected by salt-and-pepper (impulse) noise; see (**Figure 4a**). Using simple, histogram-based thresholding for segmentation of the root canal may lead to improper root canal recognition as it can be seen in (**Figure 4b**). Thus, this noise should be filtered in the pre-processing phase of the image processing, before the segmentation of the root canal. Median filters may efficiently eliminate this kind of noise; see (**Figure 4c**). Gauss filters are also useful tools to filter out this kind of noise and make the image smoother; see (**Figure 5a, b**).
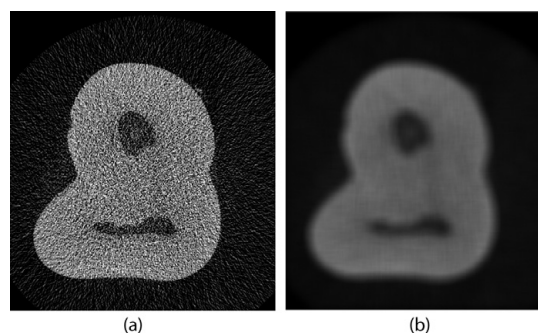
Visual representation of the segmented root canals extracted from 3D CBCT images is challenging. Point cloud visualization is a frequently used method for the
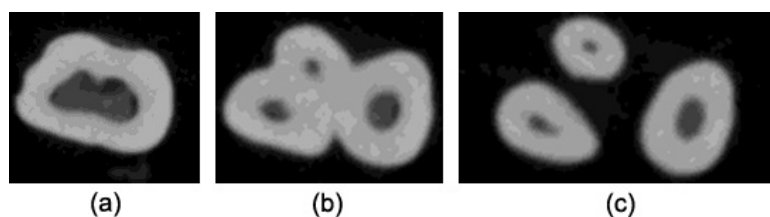
Figure 3.
*Slices of CBCT images with cross section of different sections (a, b, and c) of the root canal.*
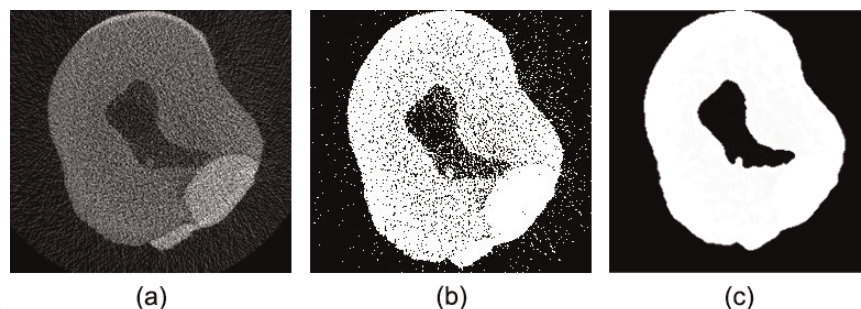
Figure 4.
A 2D slice of a CBCT image affected by salt-and-pepper (impulse) noise. (a) Original image; (b) improper root canal recognition in the original image as a result of thresholding without filtering the noise; and (c) segmentation after median filtering.
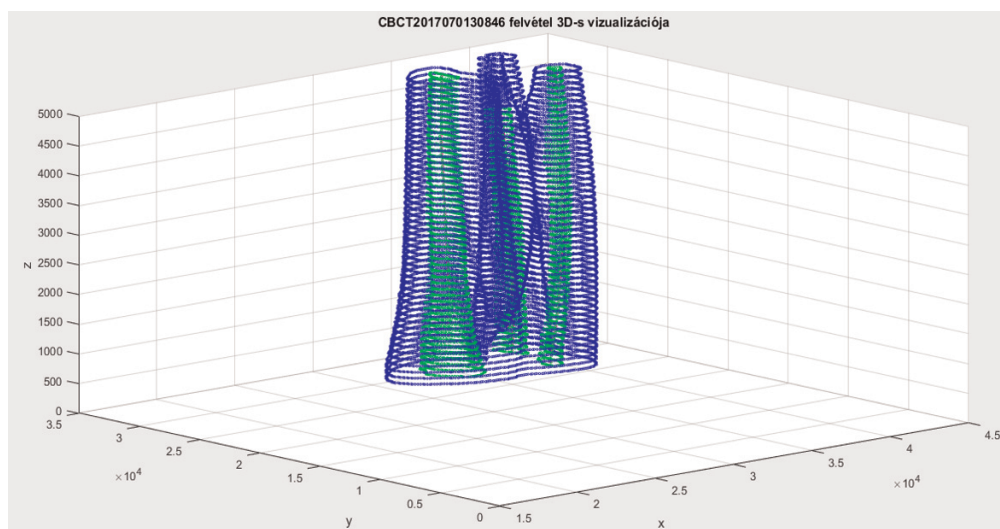

Figure 5.
Application of gauss filter on a CBCT image. (a) Original image with noise; (b) image after the application of the gauss filter.

visual interpretation of the tooth and the segmented root canal. **Figure 6a-c** are typical examples for point cloud-based visualization of the tooth.

Direct visualization of the segmented 2D images also provides the way for the representation of the segmented 3D structure of the tooth; see (**Figure 7**). The visual appearance of these 3D data sets can be improved by standard surface fitting algorithms like marching cubes method; see (**Figure 8a, b**).

(a)   (b)   (c)
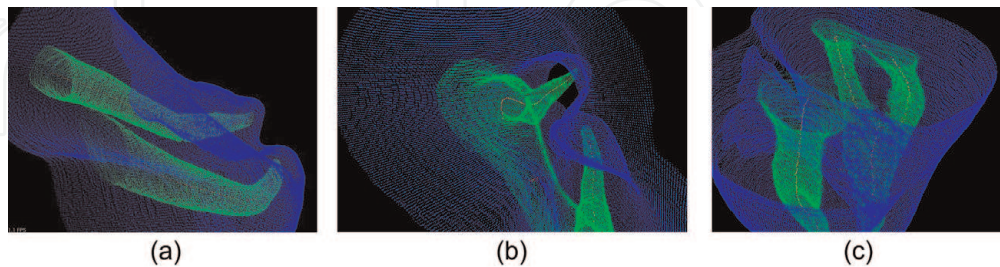
Figure 6.
Point cloud visualization of the 3D data set representing the tooth and the segmented root canal. Three different views (a), (b) and (c) of a tooth with two root canals.

Figure 7.
*Direct visualization of a 3D data set created from 2D segmented root canals.*

(a)   (b)
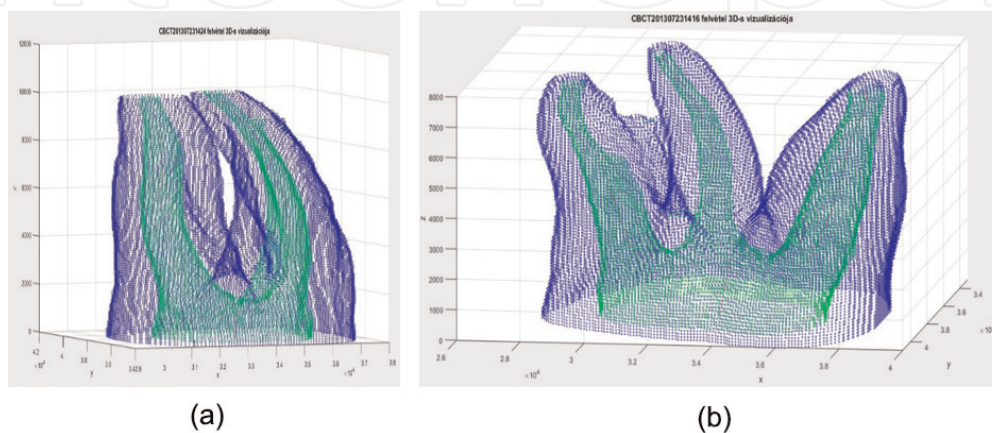
Figure 8.
3D surfaces created from segmented 2D slices by the marching cubes method. (a) A tooth with three root canals; (b) a tooth with two root canals.

6. Lessons from micro-computed tomography image analysis on extracted teeth

In a paper published in 1990 [39], μCT usability for endodontic purposes was estimated. Limited usefulness of this technique has been found in endodontics because of its high cost and of lack of adequate software available at that time. Five years later, attempts to incorporate μCT in endodontic research had been made successfully [13, 40, 41]. A consensus was made that μCT was a noninvasive technique that can accurately visualize detailed comparative data on pre- and post-instrumented canals. In an enthusiastic early study reported [13] "tremendous potential" of μCT use in endodontic research. They presented the ability of μCT assessment of area and volume change through instrumentation. Cross-sectional profile analysis was used to define canal transportation due to instrumentation. When μCT rendered image area measurement on predetermined levels of cross-section images and video-digitized physical cross-sections of root canal μCT were compared, the former was proved to be an accurate and reliable tool for experimental endodontology [41]. They also called attention to the underestimated internal area and overestimated external area measurement (approximately 3%) which was explained by the incorrect threshold determination. Bergmans and co-workers [42] used three types of software in their root canal instrumentation study. They used a volume visualization package that provided three-dimensional rendering of external and internal structure, although these renderings were not really suitable for quantitative examinations. Since the same reposition of pre and post-instrumented roots is not possible, a medical image fusion software was used for solution. This software allowed image volume alignment with subvoxel accuracy. This software analysis allowed three-dimensional root canal central axis from μCT scans. Axis was calculated by fitting a spline curve through the geometric means of wall contours on each individual slice. Application of Frenet-Serret co-ordinate frame numerical values of curvature and torsion of the curve at each point were provided. Comparison of pre and post-instrumentation spline curve canal transportation could be determined. Finally, they developed a software which implemented a true three-dimensional mathematical model for quantifying instrumentation changes. They calculated isosurfaces on pre- and post-volumes. The volume of removed dentine was calculated by subtracting pre-instrumented canal volume from post-instrumented canal volume. They visualized first untouched areas (canal wall areas which were not instrumented during enlargement) and their localizations. This unwanted result surprised endodontists who faced first with this problem and who had believed that during instrumentation, the entire or the most part of the root canal wall was cleaned. For representation of pre- and post-instrumentation fusion image, our image is shown (**Figure 9**) where a six-parameter fitting was made by Air5 package and an adaptive fuzzy C-means segmentation was used. Our representation shows a significant amount of infected debris deposition on untouched wall areas.

Recent studies [43–45] characterized the quality of instrumentation using some micro-morphological analysis developed for bone characterization which seems to be useful also in endodontic research in the following measures: surface area change (ΔSA), volume change (ΔV), and structure model index change (ΔSMI). Two-dimensional parameters at predetermined levels like area measurement, perimeter, roundness, and minor and major diameters were also defined. Center of mass change (CM shift) or canal center gravity change is a similar measurement to that of spine curve canal transportation as it is mentioned above.
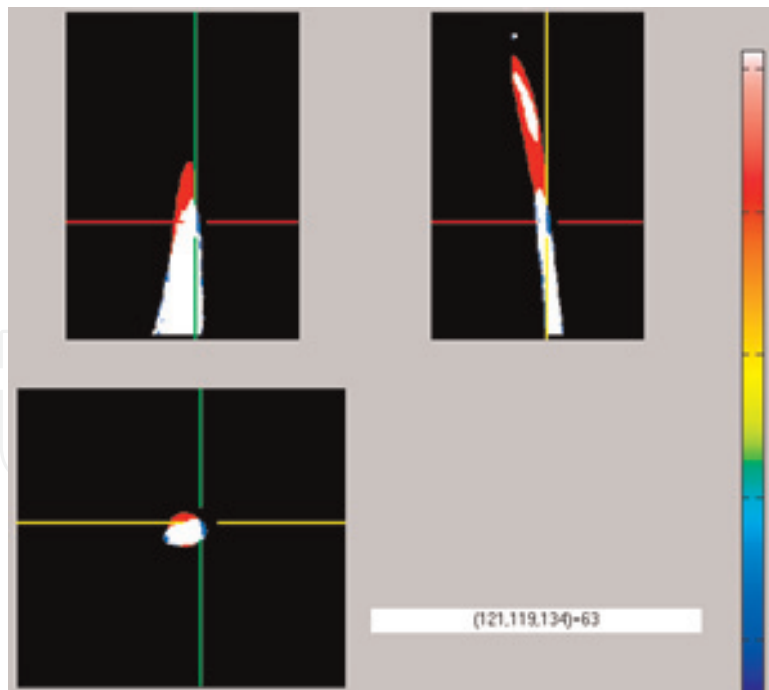
Figure 9.
A fusion image of one of our samples of pre- and post-instrumented canal in coronal sagittal and transversal views. White area represents the common part of the pre and post-instrumented canals. Red represents the enlarged part of the post-instrumented canal. Blue represents the untouched area of the original canal filled with debris.

Efficacy of residual material removal during re-treatment was assessed with μCT [46]. In a μCT study [47], it was proved that the cast post space preparation causes a higher amount of natural tooth structure loss than preparation for fiber post space.

7. Summarizing lessons gained from μCT image analysis on extracted teeth

Lesson1. Three-dimensional imaging has a great potential of studying many steps of endodontic procedures in a noninvasive manner.

Lesson 2. Recognition of the remaining high amount of untouched areas of canal wall after enlargement has turned attention of endodontists towards chemical preparation and other cleaning techniques like ultrasound or photon-induced photoacoustic streaming [24] in order to significantly improve canal preparation that will result in higher success rate of treatment expectedly.
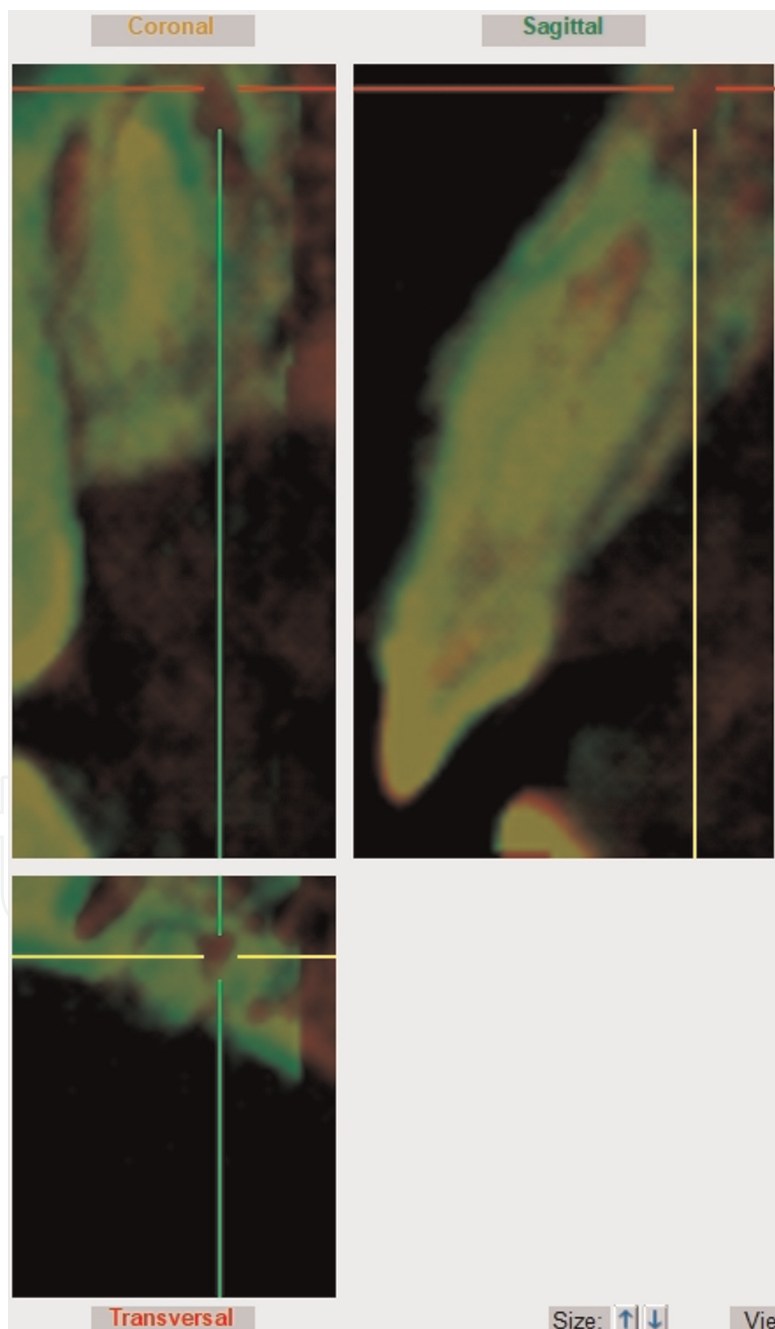

Figure 10.
Sagittal cut of a lower incisor. The dentine shows areal transparencies especially at the apical part, which refers to more calcified dentine which absorbs x-ray photons more intensely. These areal changes of density raise difficulties for automatic segmentation.

Lesson 3. Segmentation seems to be a key point of quantitative image analysis because the dentine surface density shows areal changes along the root canal (**Figure 10**).

8. Possible clinical implementation of cone beam computed tomography image analysis in endodontics

Three-dimensional image sets from high resolution (≤100 μm) CBCT equipment have a potential to be further processed in order to assess the three-dimensional axis of the main canal or main canals. Automatic segmentation of main root canal(s) and three-dimensional root canal axis determination methods have been developed. Using these available methods, endodontists now have a possibility to introduce a canal-shape classification based on the three-dimensional root canal

Figure 11.
Fusion image of healing of apical granuloma (courtesy of Professor Jozsef Varga). Periapical granuloma was visible at baseline (marked red) that was healed during several months of follow up (marked green) on CBCT scans. The apical granuloma located at the crosshair is visible as red on the fused images in all views.

axis. Among endodontist experts, a consensus is needed in classifications reflecting the demand of clinical challenges of root canal therapy like choosing a proper endodontic technique or choosing instrumentation what fits best to a given individual canal form. This kind of consensus-based software would significantly improve the success rate of endodontic therapy worldwide.

Image fusion method for pre- and post-instrumented canals in in vitro or ex vivo studies for quantitative and comparative analysis of different canal preparation equipment or techniques is widely used. At present level of technology, fused images have no clinical relevance in analyzing root canal instrumentation errors; however, there is a significant interest among endodontists in estimating the outcome of root canal therapy. Nowadays, endodontists have to wait a minimum of 6 months of recall for evaluating the success or failure of root canal therapy since periapical bone structural changes and their visualization require such a long period of time. Digital subtraction radiography (DSR) is a sensitive method; it can shorten the recall period for 1 month following root canal therapy. However, this method has not been widely spread in the field of dentistry, probably because some difficulties have arisen. The DSR technique was originally introduced in angiography and needs some extra image processing in dentistry like geometrical reconstruction and ɣ-correction of baseline and follow up radiograph pairs. An image fusion method based on three-dimensional images would be very useful, but patient's ionizing dose is still too high with CBCTs respecting the risk-benefit ratio. A CBCT image fusion case study where CBCTs were taken at endodontic treatment as baseline following a surgical treatment at some months later as follow up has already been published [49]. From the image set of this study, an apical granuloma was visible on baseline and its follow-up healing was enhanced on fuse image (**Figure 11**) presenting the possible clinical implementation of this technique.

A similar guide method used in implant surgery has been presented in some clinical endodontic cases [50, 51]. Those patients who have upper or lower incisors with obstructed and calcifically metamorphosed root canals that were not explored are potentially involved in endodontic treatment with guide. On the basis of CBCT and intra-oral scans, endodontic guides were created for the planned treatment through digital designing and rapid prototyping methods. A new artificial canal was drilled using a metal sleeve incorporated in plastic template.

Removal of adhesive fiber post avoiding root perforation, root fracture, or crack propagation is a challenge of clinicians. A three-dimensional endodontic guide method developed [52] for automatization of this procedure is increasing the success rate of less experienced dentists. Three-dimensional data from CBCT and oral cavity scanning were obtained, and computer-aided design technology generates guides with rapid prototyping to facilitate fiber post removal.

9. Limitations of novel imaging techniques and future developments

At the present level of technology, there are several limitations of CBCT equipment. CBCT is highly sensitive to movement of objects because of the small voxel size of reconstruction and of the low number of raw images used for reconstruction. In clinical situations, it is a challenge to control patient's head movements. There are some ways to improve the head movements. Supine position of the patient during scan has proven to be superior to any head support tools. Another way has been available namely an algorithm for patient movement correction. During the scan, a video capture system records the actual movements of the patient. The software analyzes and compensates for slight movements and provides improved, diagnostic quality images [53].

Another limitation of CBCTs is the development of different *artifacts* during the filtered back projection reconstruction based on Feldkamp algorithm. *Beam hardening* artifact is a real problem resulting in increased noise and misdiagnosis, for example, in root fracture. One possible solution in reducing beam hardening artifacts is application of beam hardening software. In a study where Monte Carlo analysis was used, beam hardening software reduced the beam hardening artifact errors that it was comparable with the level of error provided by synchrotron micro-CT [54].

Along with beam hardening artifact, the presence of *metal artifacts* (scatter) around the high density root canal filling material causes serious clinical diagnostic problems since the observer is unable to detect the presence of vertical root fracture [55]. Soft tissue contrast is further influenced by scatter [56]. CBCT manufacturers usually provide post-processing metal artifact reduction software and these enhancement filters have not been improved in recognition of root fracture [57]. In contrast, maximum-likelihood expectation-maximization iterative reconstruction algorithms improve the image quality and also increase signal-to-noise ratio [58]. Another way for reducing scatter significantly is introducing dual-energy imaging technology: comparison if single energy CBCT and dual-energy CBCT was dramatically reducing the metal artifact with use of upstream-filter. This method resulted also in higher signal-to-noise values [59]. First dual-energy CBCT equipment for clinical use has recently been marketed.

Photon-counting CT is a state-of-art technology with the potential to dramatically change clinical 3D imaging. Photon-counting CTs can reduce radiation dose, reconstructing images at a higher resolution, rectifies beam-hardening artifacts, optimizes the contrast agent use, and creates opportunities for quantitative imaging relative to current CT technology [60].

One of the essential limitations of current CBCT technology in detailed root canal imaging is the *voxel size*. Among the types of so-called high resolution CBCT equipment, the voxel size is between 75 and 100 micrometer [61]. At this level, the entire root canal path can be visualized. In contrast, at lower resolution equipment with 150–250 μm voxel size, the narrowest apical part of root canals cannot be visualized [62]. The diameter of physiological foramen of human molars varies between 79 and 720 μm [63]. CBCT images are not capable of giving anatomically correct images at the apex level since the apical foramen may be smaller than the adjustable voxel.

10. Conclusion

To get perspective, we remember that the best resolution in dental imaging was 2000 μm two decades earlier (this was the resolution of Scanora panoramic equipment that provided 2 mm thick layer tomograms) and today 75 μm voxel size CBCT equipment is available in the market. If you take this into consideration, this 26-times increase along with Moore's law on exponential increase chip technology is not a futuristic idea that we have 3D imaging modality with a similar resolution to that of the present μCTs in the near future. This predicts that endodontist specialists have to be prepared for understanding knowledge on lessons from μCT, must be familiar with interpreting new information, and must be able to adapt them in clinical situations in the near future.

Conflict of interest

The authors declare that they have no conflict of interest.

Author details

Csaba Dobo-Nagy[1*] and Balazs Benyo[2]

1 Department of Oral Diagnostics, Semmelweis University, Budapest, Hungary

2 Department of Control Engineering and Information Technology, Budapest University of Technology and Economics, Budapest, Hungary

*Address all correspondence to: dobo-nagy.csaba@dent.semmelweis-univ.hu

IntechOpen

References

[1] Shrestha A, Marla V, Shrestha S, Maharjan I. Developmental anomalies affecting the morphology of teeth. Revista Sul-Brasileira de Odontologia. 2015;**12**:68-78

[2] Nagy CD, Szabo J, Szabo J. A mathematically based classification of root canal curvatures on natural human teeth. Journal of Endodontics. 1995;(11): 557-560. DOI: 10.1016/S0099-2399(06) 80985-4

[3] Ahmed HMA, Dummer PMH. A new system for classifying tooth, root and canal anomalies. International Endodontic Journal. 2018;**51**:389-404. DOI: 10.1111/iej12867

[4] Hess W. Anatomie der Wurzelkanale des menschlichen Gebisses mit Berücksichtigung der feineren Verzweigungen am Foramen apicale [habilitationsschift]. Ulrich Co: Zürich; 1917

[5] Zidell J. Classification of root canal system. In: Ingle JI, Taintor JF, editors. Endodontics. 3rd ed. Philadelphia: Lea & Febiger; 1985. pp. 557-560

[6] Nagy CD, Bernath M, Szabo J. A comparative study of six methods shaping the root canal in vitro. International Endodontic Journal. 1992; **25**:29. DOI: 10.1016/j.joen.2012.11.015

[7] Schneider SW. A comparison of canal preparations in straight and curved root canals. Oral Surgery. 1971;**32**:271-275. DOI: 10.1016/0030-4220(71)90230-1

[8] Backman C, Oswald RJ, Pitts DL. A radiographic comparison of two root canal instrumentation techniques. Journal of Endodontics. 1992;**18**:19-24. DOI: 10.1016/S0099-2399(06)81137-4

[9] Schilder H. Cleaning and shaping the root canal. Dental Clinics of North America 1974;**23**:575-592. DOI:

[10] Mayo CV, Montgomery S, Rio C. A computerized method for evaluating root canal morphology. Journal of Endodontics. 1986;**12**:2-7. DOI: 10.1016/ S0099-2399(86)80274-6

[11] Berutti E. Computerized analysis of the instrumentation of the root canal system. Journal of Endodontics. 1993;**19**: 236-238. DOI: 10.1016/S0099-2399(06) 81298-7

[12] Bauman MA, Doll GM. Spatial reproduction of the root canal system by magnetic resonance microscopy. Journal of Endodontics. 1997;**23**: 49-51. DOI: 10.1016/S0099-2399(97) 80207-5

[13] Nielsen RB, Alyassin AM, Peters DD, Carnes DL, Lancaster J. Microcomputed tomography: An advanced system for detailed endodontic research. Journal of Endodontics. 1995;**21**:561-568. DOI: 10.1016/S0099-2399(06)80986-6

[14] Dobo-Nagy C, Keszthelyi G, Szabó J, Sulyok P, Ledeczky G, Szabó J. A computerized method for mathematical description of three-dimensional root canal axis. Journal of Endodontics. 2000;(11):639-643. DOI: 10.1097/ 00004770-200011000-00002

[15] Analoui M, Krisnamurthy S, Brown C. Modeling and measurement of root canal using stereo digital radiography. In: Medical Imaging 2000: Image Display and Visualization. Vol. 3976. 2000, April. pp. 306-315. DOI: 10.1117/ 12.383053

[16] Hong SY, Dong J. 3D root canal modeling for advanced endodontic treatment. In: Smart Nondestructive Evaluation for Health Monitoring of Structural and Biological Systems. Vol. 4702. 2002, June. pp. 321-331. DOI: 10.1117/12.469891

[17] Endo M, Kobashi S, Kondo K, Hata Y. Dentistry support ultrasonic system for root canal treatment aided by fuzzy logic. In: In Systems, Man and Cybernetics, 2005 IEEE International Conference on. Vol. 2. 2005, October. pp. 1494-1499. DOI: 10.1109/ICSMC.2005.1571358

[18] Lee JK, Ha BH, Choi JH, Heo SM, Perinpanayagam H. Quantitative three-dimensional analysis of root canal curvature in maxillary first molars using micro-computed tomography. Journal of Endodontics. 2006;**32**(10): 941-945. DOI: 10.1016/j.joen.2006. 04.012

[19] Willershausen B, Kasaj A, Röhrig B, Marroquin BB. Radiographic investigation of frequency and location of root canal curvatures in human mandibular anterior incisors in vitro. Journal of Endodontics. 2008;**34**(2): 152-156. DOI: 10.1016/j.joen.2007. 09.017

[20] van Soest G, Shemesh H, Wu MK, Van der Sluis LWM, Wesselink PR. Optical coherence tomography for endodontic imaging. In: Lasers in Dentistry XIV. Vol. 6843. 2008. p. 68430F. DOI: 10.1117/12.761196

[21] Germans DM, Spoelder HJ, Renambot L, Bal HE, van Daatselaar S, van der Stelt P. Measuring in virtual reality: A case study in dentistry. IEEE Transactions on Instrumentation and Measurement. 2008;**57**(6):1177-1184. DOI: 10.1109/TIM.2008.915952

[22] Park JW, Lee JK, Ha BH, Choi JH, Perinpanayagam H. Three-dimensional analysis of maxillary first molar mesiobuccal root canal configuration and curvature using micro-computed tomography. Oral Surgery, Oral Medicine, Oral Pathology, Oral Radiology, and Endodontology. 2009; **108**(3):437-442. DOI: 10.1016/j. tripleo.2009.01.022

[23] Neves ADA, Coutinho E, Cardoso MV, Jaecques SV, Van Meerbeek B. Micro-CT based quantitative evaluation of caries excavation. Dental Materials. 2010;**26**(6):579-588. DOI: 10.1016/j. dental.2010.01.012

[24] Verma P, Love RM. A micro CT study of the mesiobuccal root canal morphology of the maxillary first molar tooth. International Endodontic Journal. 2011;**44**(3):210-217. DOI: 10.1111/ j.1365-2591.2010.01800.x

[25] Yamada M, Ide Y, Matsunaga S, Kato H, Nakagawa KI. Three-dimensional analysis of mesiobuccal root canal of Japanese maxillary first molar using micro-CT. The Bulletin of Tokyo Dental College. 2011;**52**(2): 77-84

[26] Kaya S, Adiguzel O, Yavuz I, Tumen EC, Akkus Z. Cone-beam dental computerized tomography for evaluating changes of aging in the dimensions central superior incisor root canals. Medicina Oral, Patología Oral y Cirugía Bucal. 2011;**16**(3):e463-e466

[27] Li KZ, Gao Y, Zhang R, Hu T, Guo B. The effect of a manual instrumentation technique on five types of premolar root canal geometry assessed by microcomputed tomography and three-dimensional reconstruction. BMC Medical Imaging. 2011;**11**(1):14. DOI: 10.1186/1471-2342-11-14

[28] Frisardi G, Chessa G, Barone S, Paoli A, Razionale A, Frisardi F. Integration of 3D anatomical data obtained by CT imaging and 3D optical scanning for computer aided implant surgery. BMC Medical Imaging. 2011;**11**(1):5. DOI: 10.1186/1471-2342-11-5

[29] European Commission. (2012). Radiation Protection no. 172. Cone beam CT for dental and maxillofacial radiology. Evidence-based guidelines. DOI: 10.2768/21874

[30] Szilágyi L, Szilágyi SM, Benyó Z. A modified fuzzy c-means algorithm for MR brain image segmentation. In: International Conference Image Analysis and Recognition. Berlin, Heidelberg: Springer; 2007. pp. 866-877. DOI: 10.1007/978-3-540-74260-9_77

[31] Szilágyi L, Szilágyi SM, Benyó B. Efficient inhomogeneity compensation using fuzzy c-means clustering models. Computer Methods and Programs in Biomedicine. 2012;**108**(1):80-89. DOI: 10.1016/j.cmpb.2012.01.005

[32] Benyó B. Identification of dental root canals and their medial line from micro-CT and cone-beam CT records. Biomedical Engineering Online. 2012; **11**(1):81. DOI: 10.1186/1475-925X-11-81

[33] Cornea ND, Silver D, Min P. Curve-skeleton properties, applications, and algorithms. IEEE Transactions on Visualization and Computer Graphics. 2007;**13**(3):530-548. DOI: 10.1109/TVCG.2007.1002

[34] Ma CM, Sonka M. A fully parallel 3D thinning algorithm and its applications. Computer Vision and Image Understanding. 1996; **64**(3):420-433. DOI: 10.1006/cviu.1996.0069

[35] Palágyi K, Kuba A. A parallel 3D 12-subiteration thinning algorithm. Graphical Models and Image Processing. 1999;**61**(4):199-221. DOI: 10.1006/gmip.1999.0498

[36] Pudney C. Distance-ordered homotopic thinning: A skeletonization algorithm for 3D digital images. Computer Vision and Image Understanding. 1998;**72**(3):404-413. DOI: 10.1006/cviu.1998.0680

[37] Wu FC, Ma WC, Liang RH, Chen BY, Ouhyoung M. Domain connected graph: The skeleton of a closed 3D shape for animation. The Visual Computer. 2006;**22**(2):117-135. DOI: 10.1007/s00371-005-0357-4

[38] Cornea ND, Silver D, Yuan X, Balasubramanian R. Computing hierarchical curve-skeletons of 3D objects. The Visual Computer. 2005; **21**(11):945-955. DOI: 10.1007/s00371-005-0308-0

[39] Tachibana H, Matsumoto K. Applicability of X-ray computerized tomography in endodontics. Endodontics & Dental Traumatology. 1990;**6**:16-20. DOI: 10.1111/j.1600-9657.1990.tb00381.x

[40] Gambill JM, Alder M, del Rio CE. Comparison of nickel-titanium and stainless steel hand-file instrumentation using computed tomography. Journal of Endodontics. 1996;**22**:369-375. DOI: 10.1016/S0099-2399(96)80221-4

[41] Rhodes SJ, Ford Pitt RT, Lynch AJ, Liepins JP, Curtis VR. Micro-computed tomography: A new tool for experimental endodontology. International Endodontic Journal. 1999; **32**:165-170. DOI: 10.1046/j.1365-2591.1999.00204.x

[42] Bergmans L, Van Cleynenbreugel J, Wevers M, Lambrechts P. A methodology for quantitative evaluation of root canal instrumentation using microcomputed tomography. International Endodontic Journal. 2001; **34**:390-398. DOI: 10.1046/j.1365-2591.2001.00413.x

[43] Zuolo ML, Zaia AA, Belladonna FG, Silva EJNL, Souza EM, Versiani MA, et al. Micro-CT assessment of the shaping ability of four root canal instrumentation system in oval-shaped canals. International Endodontic Journal. 2018;**51**:564-571. DOI: 10.1111/iej.12810

[44] Versiani AM, Carvalho KTK, Mazzi-Chaves FJ, Manoal D, Sousa-Neto DM. Micro-computed tomographic evaluation of the shaping ability of XP-endo shaper, iRaCe, and edgefile system in long oval-shaped canals. Journal of

Endodontics. 2018;**44**:489-495. DOI: 10.1016/j.joen.2017.09.008

[45] Marceliano-Alves MFV, Sousa-Neto MD, Fidel SR, Steier L, Robinson JP, Pécora JD, et al. Shaping ability of single-file reciprocating and heat-treated multifile rotary systems: A micro-CT study. International Endodontic Journal. 2015;**48**:1129-1136. DOI: 10.1111/iej.12412

[46] Roggendorf JM, Legner M, Eberrt J, Fillery E, Frankerberger R, Friedman S. Micro-CT evaluation of residual material in canals filled with Activ GP or GuttaFlow following removal with NiTi instruments. International Endodontic Journal. 2010;**43**:200-209. DOI: 10.1111/j.1365-2591.2009.01659.x

[47] Ikram HO, Patel S, Sauro S, Mannocci F. Micro-computed tomography of tooth tissue volume changes following endodontic procedures and post space preparation. International Endodontic Journal. 2009;**42**:1071-1076. DOI: 10.1111/j.1365-2591.2009.01632.x

[48] Peters OA, Bardsley S, Fong J, Pandher G, Divito E. Disinfection of root canals with photon-initiated photoacoustic streaming. Journal of Endodontics. 2011;**37**:1008-1012. DOI: 10.1016/j.joen.2011.03.016

[49] Mensch K, Simonffy L, Cs D, Szabó BT, Varga J, Juhász A, et al. Endodontic and microsurgical treatments of maxillary lateral incisor dens invaginatus in combination with cone-beam-computed tomography fusion imaging. Oral Radiology. 2017;**33**:147. DOI: 10.1007/s11282-016-0257-5

[50] van der Meer WJ, Vissink A, Ng YL, Gulabivala K. 3D computer aided treatment planning in endodontics. Journal of Dentistry. 2016;**45**:67-72. DOI: 10.1016/j.jdent.2015.11.007

[51] Connert T, Zehnder SM, Weiger R, Kühl S, Krastl G. Microguided endodontics: Accuracy of a miniaturized technique for apically extended access cavity preparation in anterior teeth. Journal of Endodontics. 2017;**5**:1-4. DOI: 10.1016/j.joen.2016.12.016

[52] Maia LM, Júnior Moreira G, Albuquerque RC, Machado VC, Silva NRFA, Hauss DD, et al. Tree-dimensional endodontic guide for adhesive fiber post removal: A dental technique. The Journal of Prosthetic Dentistry. in press 2018. DOI: 10.1016/j.prosdent.2018.07.011

[53] Spin-Neto R, Matzen LH, Schropp L, Gotfredsen E, Wenzel A. Factors affecting patient movement and re-exposure incone beam computed tomography examination. Oral Surgery, Oral Medicine, Oral Pathology, Oral Radiology. 2015;**119**:572-578. DOI: 10.1016/j.oooo.2015.01.011

[54] Kovács M, Danyi R, Erdélyi M, Fejérdy P, Dobo-Nagy C. Distortional effect of beam-hardening artefacts on microCT: A simulation study based on an in vitro caries model. Oral Surgery, Oral Medicine, Oral Pathology, Oral Radiology, and Endodontics. 2009;**108**:591-599. DOI: 10.1016/j.tripleo.2009.06.009

[55] Kovács M, Fejérdy P, Nagy Cs D. A fém műtermék a fejnyaki cone-beam CT (CBCT) képeken. Fogorvosi Szemle. 2008;**5**:171-178

[56] Tofts PS, Gore JC. Some sources of artefact in computed tomography. Physics in Medicine and Biology. 1980;**25**:117-127

[57] Ferreira JB, Christovam IO, Alencar DS, da Motta AFJ, Mattos CT, Cury-Saramago A. Accuracy and reproducibility of dental measurements on tomogrphic digital models: A systematic review and meta-analysis. Dento Maxillo Facial Radiology. 2017;**46**:20160455. DOI: 10.1259/dmfr.20160455

[58] Bechara BB, Moore WS, McMahan CA, Noujeim M. Metal artefact reduction with cone beam CT: An in vitro study. Dento Maxillo Facial Radiology. 2012;**41**:248-253. DOI: 10.1259/dmfr/80899839

[59] Iramina H, Hamaguchi T, Nakamura M, Mizowaki T, Kanno I. Metal artifact reduction by filter-based dual-energy cone-beam computed tomography on a bench-top micro-CBCT system: Concept and demonstration. Journal of Radiation Research. 2018;**59**:511-520. DOI: 10.1093/jrr/rry034

[60] Willemink JM, Pourmorteza A, Pelc JN, Fleischmann D. Photon-counting CT: Technical principles and clinical prospects. Radiology. 2018;**289**:293-312. DOI: 10.1148/radiol.2018172656

[61] Kiljunen T, Kaasalainen T, Suomalainen A, Kortesniemi M. Dental cone beam CT: A review. Physica Medica. 2015;**31**:844-860. DOI: 10.1016/j.ejmp.2015.09.004

[62] Szabó BT, Pataky L, Mikusi R, Fejérdy P, Dobo-Nagy C. Comparative evaluation of cone-beam CT equipment with micro-CT in the visualization of root canal system. Annali Dell'Istituto Superiore Di Sanitá. 2012;**48**:49-52. DOI: 10.4415/ANN_12_01_08

[63] Abarca J, Zaror C, Monardes H. Morphology of the physiological apical foramen in maxillary and mandibular first molars. International Journal of Morphology. 2014;**32**:671-677. DOI: 10.4067/S0717-95022014000200048